*33rd EPS Conference on Plasma Phys. Rome, 19 - 23 June 2006 ECA Vol.**30I**, P-1.002 (2006)*

Numerical Simulation of Imploding Cylindrical Laser-Targets

R. Ramis[1], J. Ramírez[1] and G. Schurtz[2]

[1] *E.T.S.I. Aeronáuticos, Universidad Politécnica de Madrid (SPAIN)*

[2] *CELIA, Université Bordeaux 1 (FRANCE)*

Experiments with cylindrical targets allow to study the basic physics of the implosion process of inertial fusion capsules driven by either indirect (Hsing *et al.*, 1997) or direct (Tubbs *et al.*, 1999; Barnes *et al.*, 2002; Lanier *et al.*, 2003; Parker *et al.*, 2004; Finckle *et al.*, 2004 and 2005) irradiation. This geometry allows the observation of the target interior by means of axial diagnostics and, at the same time, retains important physical phenomena, like the Bell-Pleset effect, not present in planar experiments. The upgrade of the LIL (Ligne d'Intégration Laser) (Kovacs, 2002 and www-lmj.cea.fr) to eight beams, called OCTALIL, with a total energy of 50 kJ in 5 ns, will take place around 2008, and will allow to shot to this sort of configurations. By the same time, a 3 kJ, 1 ps laser, now under development, will be available in the target chamber, and could be used to generate high resolution diagnostic sources, like proton or fast X ray radiography. We consider a target (see figure 1) composed of a cylindrical $(CH_2)_n$ shell with 0.06 cm internal radius and 0.003 cm thickness, filled with deuterium gas at 30 bars. This target will be irradiated with the eight blue beams of the OCTALIL laser system arranged in an approximately octahedrical configuration. Although, in principle, the process is three-dimensional, we can extract useful information from currently available two-dimensional simulations. We have used the code MULTI (Ramis *et al.*, 1988; 2004; and server.faia.upm.es/multi) to study both, the transversal (R-θ geometry) and longitudinal (R-Z geometry) sections of the cylindrical target, as well as the 1D averaged problem. Figure 2A shows schematically the setting of the R-Z simulations. We use a pure Lagrangian grid with 12+64 cells in radial direction to describe the filling gas and the ablator, and 32 cells in longitudinal direction. The target is irradiated by beams with super-Gaussian intensity profiles: $I \propto e^{-\left((x/a)^2+(y/b)^2\right)^m}$, where x and y are orthogonal coordinates perpendicular to the center line of the beam. Typically we have $a \geq b$; beam section is elongated along the direction of target

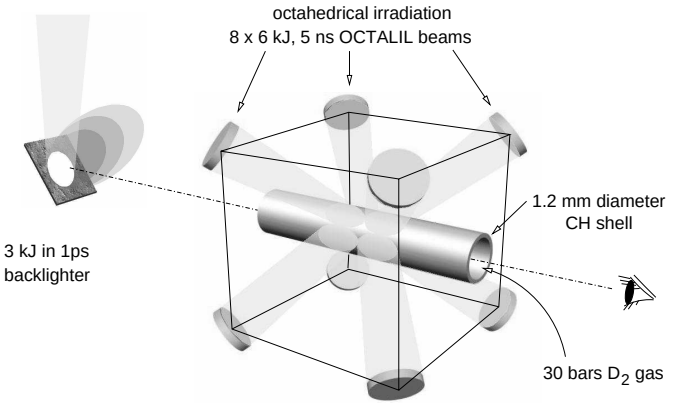

Figure 1: OCTALIL cylindrical target

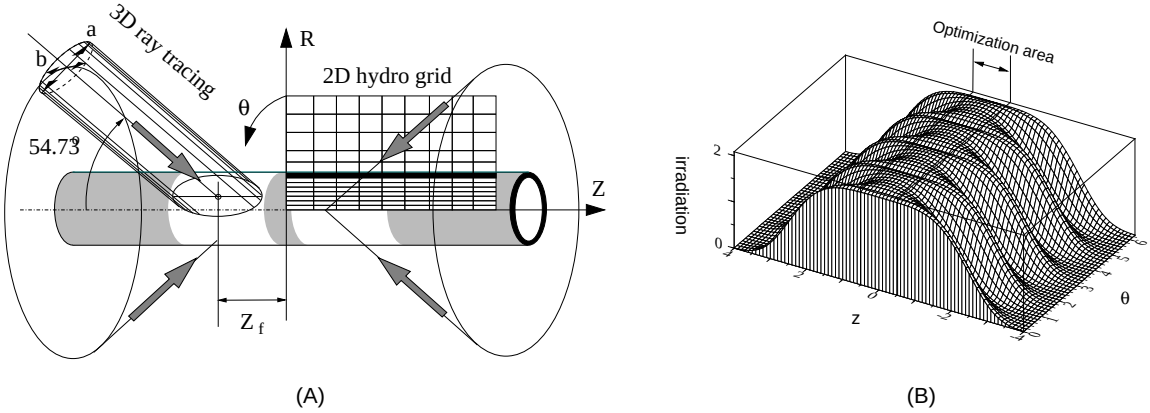

Figure 2: Irradiation scheme and static irradiation pattern

axis. The laser center lines intersect the initial surface of the cylinder at an angle of 55^o from the axis, at a distance Z_f from target equator. Hydrodynamic and radiation quantities are assumed

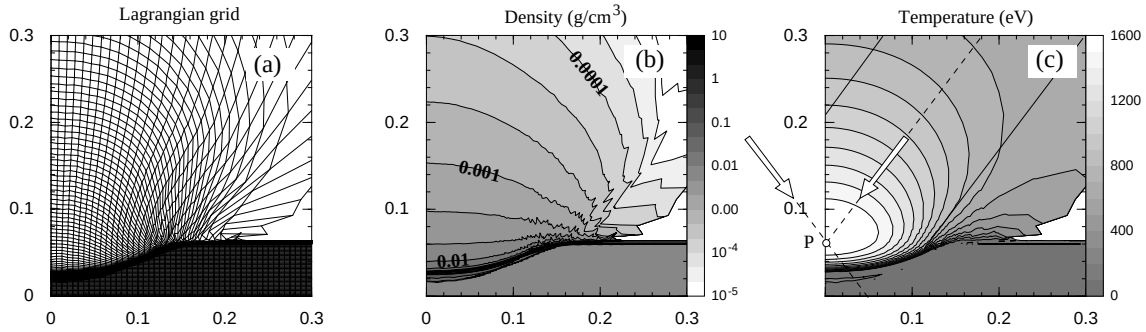

Figure 3: Snapshot of a longitudinal simulation at 4 ns

to be not depending on the the cylindrical θ coordinate. Laser deposition, computed in 3D, is averaged in θ direction in order to be coupled with hydrodynamics. The static irradiation pattern, obtained by neglecting hydro-motion and assuming total absorption, has been previously optimized (Schurtz, 2004). For a cylinder of a given radius r, the values of a, b, m and $Z_f = 0$ have been chosen to maximize the uniformity in the central part of the cylinder with a length equal to the radius (see figure 2B). For $a = 1.86 \times r$, $b = 0.93 \times r$, $m = 2.2$ and $Z_f = 0$ one has 1.12 % of RMS non-uniformity. Figure 3 shows a snapshot of an R-Z simulation using the above described irradiation, 4 ns after beginning of the pulse, when the central part of the cylinder has imploded to about one half of its initial diameter. The numerical grid moving with the fluid is drawn in inset (a), showing a regular structure in the region of interest: the central part of the target. Isodensity contours are presented in inset (b); the critical surface with 0.028 g cm^{-3} is

very close to the ablation surface. Finally, inset (c) shows the matter isotherms; the maximum temperature 1760 eV is reached at a place close to focus point P. At the end of the implosion, the central region of the cylinder, with a length of about 0.08 cm, has been compressed up to 0.0026 cm radius, with a density of about 1.5-2.0 g cm^{-3}.

The shape of the gas-ablator interface as a function of time is presented in figure 4A. In addition of the above case, we have considered also circular focused beams ($a = b = 0.93 \times r$), probably more easy to implement in practice than an elliptical focus. We have simulated different configurations, with Z_f ranging from -0.1 cm to 0.1 cm. With $Z_f \simeq 0$, the initial focal spots of left and right sides coincide, producing a strong and concentrated implosion (See figure 4B). By using $Z_f \simeq -0.055$ cm, the laser beams cross each other and the focal spots of both sides overlap in such a manner that the longitudinal uniformity is maximized. A filamentary compressed region of 0.16 cm length is then produced. The compression is up to 0.003 cm radius with a density of about 1.5-2.0 g cm^{-3}. (figure 4C). This configuration appears to be very favorable in terms of longitudinal uniformity. Finally, for larger separations between the two beam-cones, a double spot compression is produced (figure 4D). Some of the performances of the target can be evaluated through the 1D analysis of the cylindrically symmetric implosion of a representative section of the target of length L. We perform several 1D simulations with different values of L (that is, different intensities) until the implosion time agrees with the value of 2D simulations at the central section of the cylinder. In this way, we obtained $L \simeq 2$ mm for the cases of interest. Temperature (electron and radiation), pressure and density profiles are shown in figure 5 (left) at the moment of maximum compression. In this figure, it is visible the ablation of the internal side of the plastic ablator by a radiative thermal wave driven by the radiation generated by the very hot deuterium plasma. The central hot spot is optically thin and its radiation temperature ($\simeq$380 eV) is determined by the temperature reached in the surrounding plastic ablator. Finally, we have checked the sensibility of the results to several modelling details: opacity, thermal flux

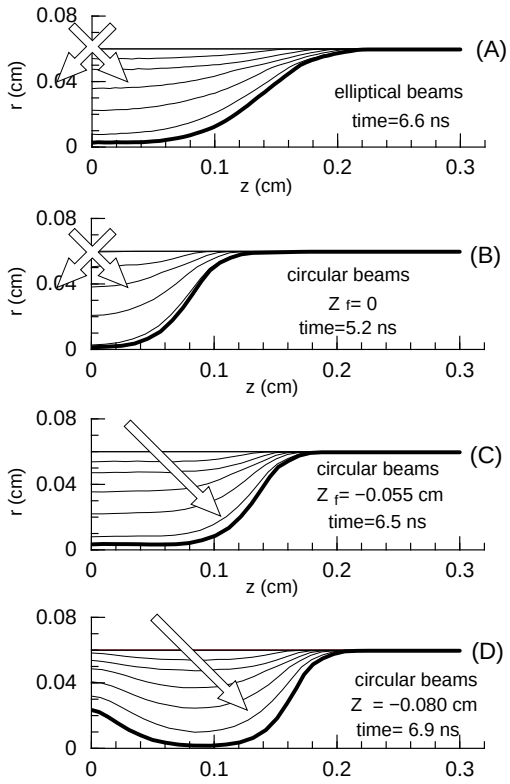

Figure 4: Evolution of the gas-ablator interface.

inhibition, grid resolution, ... The radiation transport role has been checked by switching out radiative transport in the simulations (figure 5 (right)). Global characteristics of plasma blowoff

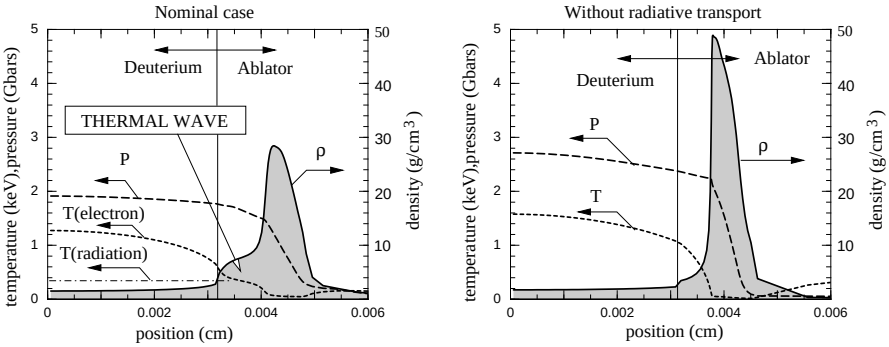

Figure 5: Final compressed configuration with and without radiative transport enabled

are similar, but due to the absence of radiative losses (6.6 % of laser energy), the implossion velocity is larger (18.5×10^6 cm s^{-1} versus 17.6×10^6 cm s^{-1}). The absence of the the thermal wave feature produces a larger temperature in deuterium, and, despite the pressure is a factor 1.38 larger, the average density of deuterium is practically the same (just a 3% more) in both cases. By the other hand, the preheating of the ablator by radiation reduces its density. This research has been supported by CICYT of Spain projects FTN 2003-06901, FTN 2001-3845, HF03-186 (Acción Integrada), and by EURATOM/CIEMAT association in the framework of the 'IFE Keep-in-Touch Activities'.

REFERENCES

Barnes, C.W., *et al.*, (1002) Phys. Plasmas **(**9) 4431.

Fincke, J.R., *et al.*, (2004) Phys. Rev. Letts. **93**, 115003, and (2005) Laser Part. Beams **23**, 21.

Hsing, W.W., *et al.*, (1997) Phys. Plasmas **4**, 1832, and (1997) Phys. Rev. Letts. **78**, 3876.

Kovacs, F., *"LIL: Status and Commissioning"* (2002), in Proceedings of the IFSA 2001, edited by K.A. Tanaka, D.D. Meyerhofer and J. Meyer-ter-Vehn, Elsevier, Paris, pp-484-489

Lanier, N.E., *et al.*, (2003) Phys. Plasmas **10**, 1816.

Parker, K., *et al.*, (2004) Phys. Plasmas **11**, 2696.

Ramis, R., *et al.*, (1988) Comp. Phys. Comm. **49**, 475, and (2004) Nucl. Fusion **44**, 720.

Tubbs, D.L., *et al.*, (1999) Laser Part. Beams **17**, 437, and (1999) Phys. Plasmas **6**, 2095.

Schurtz, G., *"FCI par attaque directe. Utilisation de la LIL en configuration éclatée ou LIL 6+2"* (2004) CELIA Report, TALENCE, France.